THE JOURNAL OF BIOLOGICAL CHEMISTRY VOL. 290, NO. 25, pp. 15855–15865, June 19, 2015

Functional Architecture of the Cytoplasmic Entrance to the Cystic Fibrosis Transmembrane Conductance Regulator Chloride Channel Pore*

Received for publication, March 31, 2015, and in revised form, April 24, 2015 Published, JBC Papers in Press, May 5, 2015, DOI 10.1074/jbc.M115.656181

Yassine El Hiani and Paul Linsdell[1]

From the Department of Physiology and Biophysics, Dalhousie University, Halifax, Nova Scotia B3H 4R2, Canada

Background: The cytoplasmic entrance to the CFTR channel pore is not defined.
Results: Functionally important positively charged amino acid side chains attract Cl^- to the cytoplasmic entrance to the pore.
Conclusion: A lateral portal leads to the inner mouth of the pore.
Significance: This work defines the last unknown region of the anion permeation pathway.

As an ion channel, the cystic fibrosis transmembrane conductance regulator must form a continuous pathway for the movement of Cl^- and other anions between the cytoplasm and the extracellular solution. Both the structure and the function of the membrane-spanning part of this pathway are well defined. In contrast, the structure of the pathway that connects the cytoplasm to the membrane-spanning regions is unknown, and functional roles for different parts of the protein forming this pathway have not been described. We used patch clamp recording and substituted cysteine accessibility mutagenesis to identify positively charged amino acid side chains that attract cytoplasmic Cl^- ions to the inner mouth of the pore. Our results indicate that the side chains of Lys-190, Arg-248, Arg-303, Lys-370, Lys-1041, and Arg-1048, located in different intracellular loops of the protein, play important roles in the electrostatic attraction of Cl^- ions. Mutation and covalent modification of these residues have charge-dependent effects on the rate of Cl^- permeation, demonstrating their functional role in maximization of Cl^- flux. Other nearby positively charged side chains were not involved in electrostatic interactions with Cl^-. The location of these Cl^--attractive residues suggests that cytoplasmic Cl^- ions enter the pore via a lateral portal located between the cytoplasmic extensions to the fourth and sixth transmembrane helices; a secondary, functionally less relevant portal might exist between the extensions to the 10th and 12th transmembrane helices. These results define the cytoplasmic mouth of the pore and show how it attracts Cl^- ions from the cytoplasm.

Cystic fibrosis is caused by mutations in a single gene that cause loss of function of the cystic fibrosis transmembrane conductance regulator (CFTR),[2] an epithelial cell Cl^- channel (1). CFTR is a member of the large ATP-binding cassette (ABC) family of transport ATPases (2) but is unique within this family in acting as an ion channel rather than an active transport protein. All ABC proteins exhibit a modular architecture with two cytoplasmic nucleotide binding domains (NBDs) that hydrolyze ATP coupled to two membrane-spanning domains (MSDs) that form the substrate transport pathway (Fig. 1, *A* and *B*). In CFTR, the NBDs control ATP-dependent gating of the transmembrane Cl^- channel pore (3), which is formed by a subset of the 12 transmembrane segments (TMs) (4). The TMs are joined by short extracellular loops exposed to the exterior of the cell and longer intracellular loops (ICLs) that extend into the cytoplasm and form a structural and functional link between the NBDs and MSDs (Fig. 1, *A* and *B*). CFTR also contains a unique cytoplasmic regulatory or R domain that is the site of channel regulation by phosphorylation and dephosphorylation (3).

The structure of full-length CFTR has been observed directly only at low resolution (5). However, several atomic level homology models have been developed based on related, non-ion channel ABC protein templates (6, 7) (Fig. 1*B*). The ability of these models to represent accurately the MSDs, which are the region of highest structural and functional diversity between CFTR and the templates used, has been criticized (4). Nevertheless, continuing refinement of these models means that there is now good agreement between structural models of the MSDs (6, 7) and functional data from a wealth of structure-function (4) and substituted cysteine accessibility mutagenesis studies (8) of the Cl^- channel pore. As a result, the overall shape of a continuous central Cl^- permeation pathway from the extracellular solution to the innermost extent of the TMs, lined by TMs 1, 6, 11, and 12, is well established (Fig. 1*B*). However, how this pathway then connects to the cytoplasm is not apparent in current structural models (6, 7), and at the same time, there are almost no functional data concerning the pathway taken by Cl^- ions as they pass between the cytoplasm and the central pore formed by the TMs (Fig. 1*C*). It is clear from molecular models that much of what is referred to as the ICLs are in fact cytoplasmic extensions of the TM α-helices with shorter "coupling helices" at the cytoplasmic ends of the ICLs forming a connection to the NBDs (Fig. 1*B*). Early homology modeling

* This work was supported by the Canadian Institutes of Health Research.
[1] To whom correspondence should be addressed: Dept. of Physiology and Biophysics, Dalhousie University, P. O. Box 15000, Halifax, Nova Scotia B3H 4R2, Canada. Tel.: 902-494-2265; Fax: 902-494-1685; E-mail: paul.linsdell@dal.ca.
[2] The abbreviations used are: CFTR, cystic fibrosis transmembrane conductance regulator; ABC, ATP-binding cassette; ICL, intracellular loop; MSD, membrane-spanning domain; MTS, methanethiosulfonate; MTSES, [2-sulfonatoethyl]MTS; MTSET, [2-(trimethylammonium)ethyl]MTS; NBD, nucleotide binding domain; TM, transmembrane segment.

suggested that the TM extensions that make up the ICLs may form a narrow central "funnel" that forms a pathway for Cl^- movement between the cytoplasm and the transmembrane pore formed by the TMs (9, 10). However, such a funnel model was not supported by experiments investigating the functional effects of mutations within the ICLs on Cl^- permeation (11, 12). The cytoplasmic entrance to the pore therefore remains the final unexplored region of the Cl^- permeation pathway. The goal of the current study was to obtain functional evidence for the identity of functionally important amino acid residues located close to the cytoplasmic entrance to the pore.

Recent molecular modeling and molecular dynamics simulations have suggested a novel alternative structure to the cytoplasmic aspect of the Cl^- permeation pathway (7). Thus, it was suggested that Cl^- ions enter the central pore via at least one and potentially up to four lateral portals or tunnels formed by the TM cytoplasmic extensions within the ICLs (7) (Fig. 1*C*). The proposed locations of these portals or "lateral tunnels," as originally described by Mornon *et al.* (7), are depicted in Fig. 1. Currently there is no functional evidence to support the existence of such portals; nevertheless, their proposed existence could be related to the intriguing observation of an apparent cytoplasmic portal observed using electron crystallography (13). Lateral cytoplasmic portals leading to a central pore have been identified in several other ion channel types (*e.g.* Refs. 14–18).

One residue has been suggested to play an important functional role close to the cytoplasmic entrance of the pore, Arg-303 at the intracellular end of TM5 (19, 20) (Fig. 1*C*). Altering the side chain charge at this position (either by mutagenesis or by covalent modification of R303C by charged cysteine-reactive methanethiosulfonate (MTS) reagents) suggested that the positive charge at this position played a key role in attracting Cl^- ions electrostatically from the cytoplasm to the inner mouth of the pore (19). The lateral portal model recently put forth by Mornon *et al.* (7) suggested that these putative cytoplasmic portals to the pore were also decorated by multiple positively charged arginine, lysine, and histidine side chains, and it was hypothesized that some of these positive charges, like that at Arg-303, could also play important functional roles in attracting cytoplasmic Cl^- ions to the pore (7). In the present work, we used cysteine substitution and *in situ* modification by negatively and positively charged MTS reagents to probe the functional roles of each of the positively charged amino acid residues proposed to be located close to the putative cytoplasmic portals. Our results suggest that one functionally dominant lateral portal located between the cytoplasmic extensions of TM4 and TM6 is the main entrance for cytoplasmic Cl^- ions to enter the pore with the possibility of another, functionally more minor portal between the extensions of TM10 and TM12. Positively charged amino acid side chains attract cytoplasmic Cl^- ions to these cytoplasmic portals, maximizing the rate of conduction.

Experimental Procedures

Experiments were carried out on baby hamster kidney cells transiently transfected with CFTR. In this study, we used a human CFTR variant in which all cysteines had been removed by mutagenesis (as described in Ref. 21) and that includes a mutation in NBD1 (V510A) to increase protein expression in the cell membrane (22). This Cys-less variant, which we have used extensively in previous studies of CFTR pore structure and function (8), has functional pore properties very similar to those of wild-type CFTR (23). Additional mutations were introduced into the Cys-less background using the QuikChange site-directed mutagenesis system (Agilent Technologies, Santa Clara, CA) and verified by DNA sequencing.

To test the functional roles of positively charged amino acid side chains located close to putative cytoplasmic portals leading to the pore, we mutated to cysteine all positively charged arginine, lysine, and histidine side chains identified by Mornon *et al.* (7) as potentially being located close to four possible portals (Fig. 1, *D* and *E*). According to this model (and as illustrated in Fig. 3 of Ref. 7), four potential cytoplasmic portals were identified between the cytoplasmic extensions to TM2 and TM11, TM4 and TM6, TM5 and TM8, and TM10 and TM12. The approximate locations of these putative portals are depicted in Fig. 1, *D* and *E*. The residues within the ICLs that were mutated in the present study were (according to TM cytoplasmic extension) Arg-153 (TM2), Lys-190 (TM3), Arg-248 (TM4), Arg-251 (TM4), Lys-254 (TM4), Lys-294 (TM5), Arg-297 (TM5), Lys-298 (TM5), Lys-370 (TM6), Lys-946 (TM8), His-949 (TM8), Arg-975 (TM9), Lys-978 (TM9), Lys-1041 (TM10), Arg-1048 (TM10), His-1085 (TM11), Arg-1162 (TM12), and Lys-1165 (TM12). For orientation, ICL1 connects the cytoplasmic ends of TMs 2 and 3, ICL2 connects TMs 4 and 5, ICL3 connects TMs 8 and 9, and ICL4 connects TMs 10 and 11 (Fig. 1*A*). We also included Arg-303 (TM5), previously identified as being close to the cytoplasmic entrance to the pore (19), as a positive control for a functionally important pore-lining positive charge.

Macroscopic and single channel recordings were made using the excised, inside-out configuration of the patch clamp technique as described in detail previously (24). For both macroscopic and single channel recordings, CFTR channels were activated after patch excision and recording of background currents by exposure to protein kinase A catalytic subunit (PKA; 20 nM) and MgATP (1 mM) in the cytoplasmic solution. For macroscopic current recordings, both the intracellular (bath) and extracellular (pipette) solution contained 150 mM NaCl, 2 mM $MgCl_2$, 10 mM *N*-tris-[hydroxymethyl]methyl-2-aminoethanesulfonate. As in a previous substituted cysteine accessibility mutagenesis study of ICL3 (11), for single channel recordings, NaCl in the pipette solution was replaced with 150 mM sodium gluconate to generate an outwardly directed Cl^- concentration gradient. The transmembrane Cl^- concentration gradient is not expected to influence any of the parameters measured in our experiments. All experimental solutions were adjusted to pH 7.4.

Current traces were filtered at 100 (for macroscopic currents) or 50 Hz (for single channel currents) using an eight-pole Bessel filter, digitized at 250 Hz, and analyzed using pCLAMP9 (Molecular Devices, Sunnyvale, CA). Pipette resistances were 1–2 megaohms for macroscopic current recording and 7–10 megaohms for single channel recording. Macroscopic current amplitudes were monitored during brief voltage ramps (to ±50

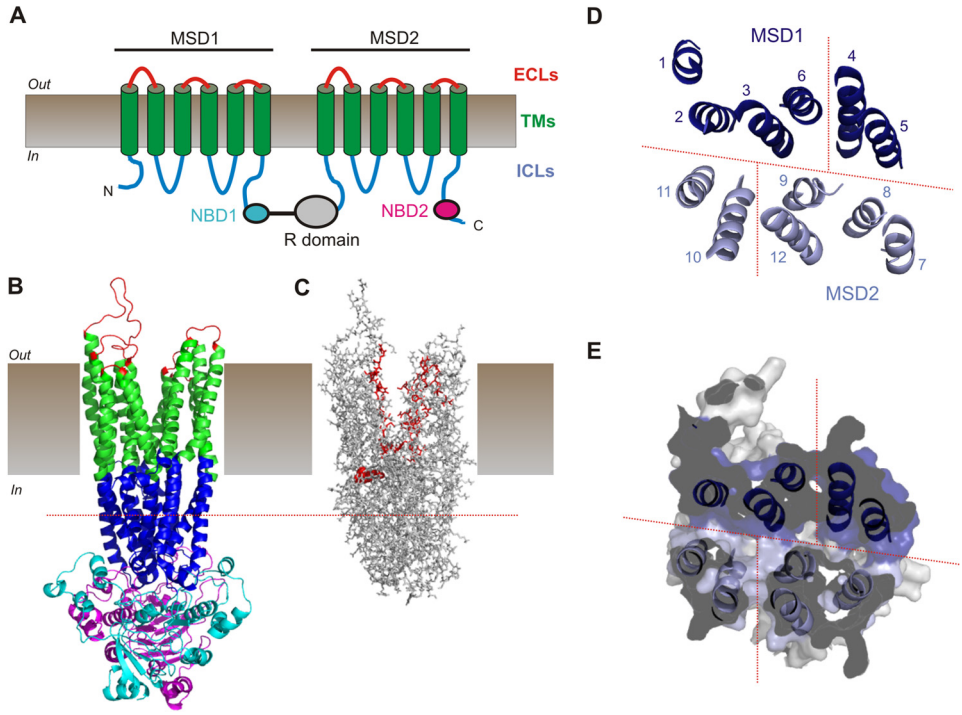

FIGURE 1. **Putative structure of the Cl^- permeation pathway in CFTR.** *A*, schematic representation of CFTR topology comprising 12 TMs (*green*), two NBDs (NBD1, *cyan*; NBD2, *magenta*), ICLs (*blue*), and extracellular loops (*ECLs*) (*red*). *B*, overall domain architecture of CFTR as presented in a recent atomic homology model based on the bacterial ABC protein Sav1866 (7). The same color scheme as in *A* illustrates the approximate extent of the different domains. The R domain is absent from this model. *C*, location of putative pore-forming amino acid side chains traces the Cl^- permeation path in this model. TMs, ICLs, and extracellular loops only (NBDs removed) are in shown in stick representation. Those amino acids in TMs 1, 6, 11, and 12 that have been proposed to line the channel pore as reviewed recently (8) are shown in *red*. These residues delineate an approximately central pore through the TMs; however, the nature or location of a pathway for Cl^- ion movement connecting the TMs to the cytoplasm is not apparent. One residue that has been proposed to contribute to the cytoplasmic aspect of the pore, Arg-303 at the intracellular end of TM5 (19), is shown in *red* as a *space-filling* representation for increased visibility. *D* and *E*, proposed location of putative "cytoplasmic portals" to the pore formed by the ICLs as originally proposed by Mornon *et al.* (see Fig. 3 in Ref. 7). *D*, the homology structure of the α-helical extensions of the TMs that make up the ICLs viewed from the membrane side is represented by the corresponding TM extension (*i.e.* "*1*" refers to the cytoplasmic extension of TM1). Mornon *et al.* (7) proposed that up to four lateral portals could connect the central pore to the cytoplasm; the approximate locations of these putative pathways are shown as *red dashed lines*. *E*, location of these putative portals in a cut-away cross-sectional view of the ICLs (see also Ref. 7). The putative portal between TMs 4 and 6 is not visible in this section and may be located slightly more toward the cytoplasmic side (7). The approximate level of this section is illustrated by the *red dashed line* in *B* and *C*. CFTR model structures (*B–E*) were visualized with PyMOL (39) using coordinates provided by Mornon *et al.* (7).

mV) from a holding potential of 0 mV applied every 6 s as described in previous studies of modification of cysteine residues in CFTR (11, 27, 28).

Channels were exposed to intracellular cysteine-reactive MTS reagents to covalently modify an introduced cysteine side chain. Two MTS reagents, the negatively charged [2-sulfonatoethyl]MTS (MTSES) and the positively charged [2-(trimethylammonium)ethyl]MTS (MTSET), were used at high concentrations (200 μM) that we have previously shown to have no effect on Cys-less CFTR (22, 25–27). MTS reagents were applied to the cytoplasmic face of inside-out patches after stable current activation with PKA and ATP. In some cases, the identity of the remaining currents as being carried by CFTR was confirmed using the CFTR-specific inhibitor $CFTR_{inh}$-172. $CFTR_{inh}$-172 was initially prepared as a high concentration stock solution (20 mM) in dimethyl sulfoxide, stored frozen at 4 °C until the time of use, diluted, and added to the experimental chamber at a final concentration of 5 μM.

Both mutations (12, 29–32) and MTS modification of cysteine side chains (11) within the ICLs frequently alter CFTR channel gating, leading to a change in overall channel open probability. The exact mechanistic origin of these effects is not clear but is consistent with the ICLs acting as a physical and functional link between the cytoplasmic NBDs and the channel gate within the MSDs (12, 32, 33). Because the present study was focused on the functional role of positively charged amino acid side chains within the ICLs in contributing to the Cl^- permeation pathway, we sought to isolate the effects of MTS modification on Cl^- permeation. Initially, we investigated macroscopic currents carried by MTS-sensitive channel mutants after treatment with intracellular sodium pyrophosphate (PP_i; 2 mM) to stabilize the channel open state (34, 35). We have previously used this approach in studies of state-dependent modification of cysteine residues introduced into Cys-less CFTR to isolate or enrich effects on open CFTR channels (27, 36, 37). Subsequently, effects of MTS modification on the rate of Cl^- permeation through open channels were investigated more directly using measurement of single channel current amplitude.

Experiments were conducted at room temperature (21–24 °C). The values are presented as the means ± S.E. Tests of significance were conducted using an unpaired *t* test with $p < 0.05$ being considered statistically significant. All chemicals were obtained from Sigma-Aldrich except for MTSES and MTSET (Toronto Research Chemicals, North York, Ontario, Canada) and PKA (Promega, Madison, WI).

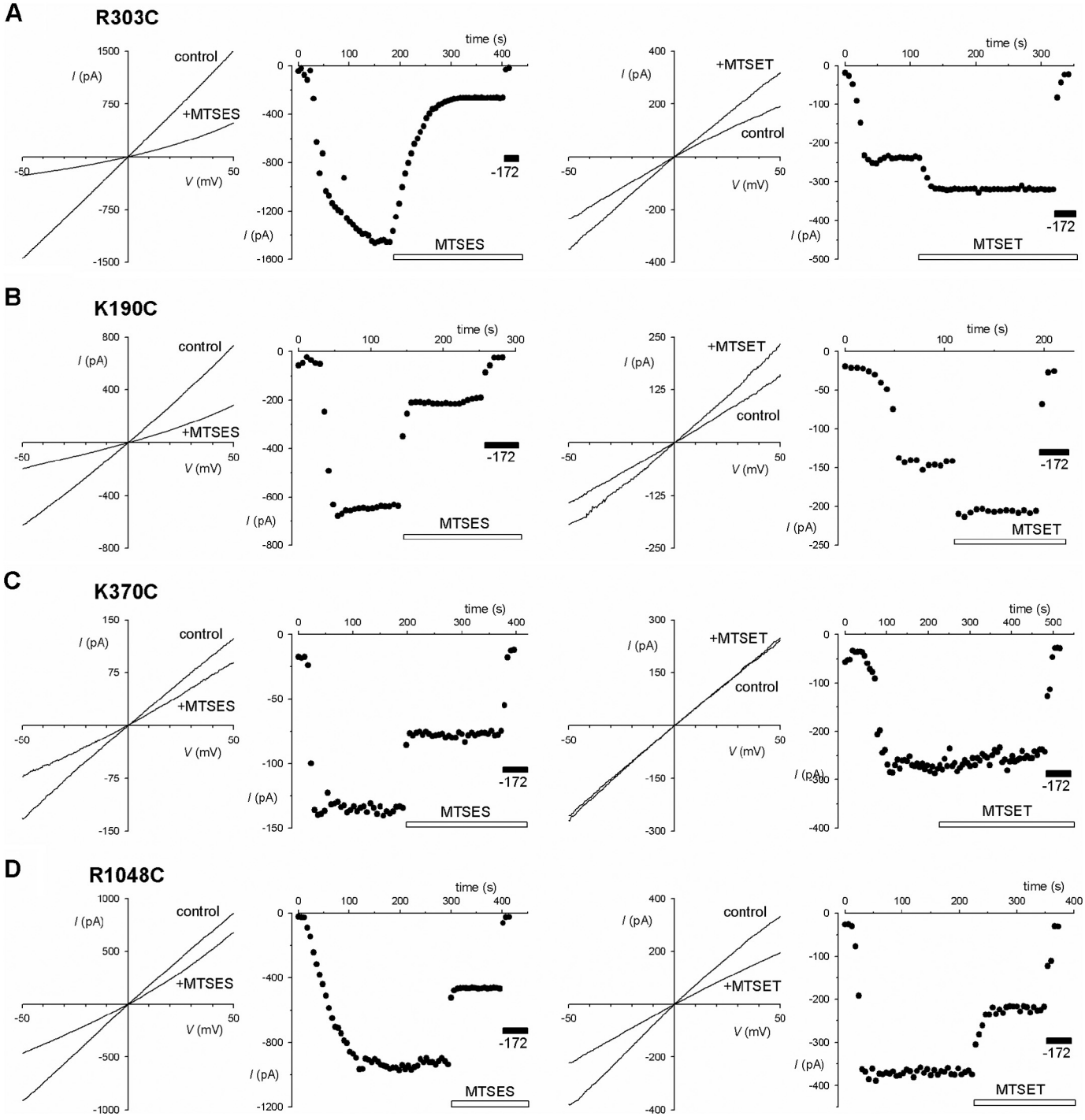

FIGURE 2. **Modification of cysteine-substituted CFTR mutants by cytoplasmically applied MTSES and MTSET.** *A–D*, examples of modification of four different mutants (*A*, R303C, used in this study as a positive control; *B*, K190C; *C*, K370C; *D*, R1048C) by MTSES (*left panels*) or MTSET (*right panels*). For each example, leak-subtracted *I-V* relationships were recorded following channel activation with PKA and ATP (control) and after addition of MTS reagent (200 μM) to the intracellular solution. Time courses of current activation (by PKA application in the presence of ATP at time 0) and MTS reagent modification (as indicated by *white bars*) are shown for the same membrane patches. The identity of CFTR currents was confirmed by sensitivity to $CFTR_{inh}$-172 (*-172*; 5 μM; indicated by *black bars*) at the end of the recording. Note that although the effect of MTSES was inhibitory in each of these mutants MTSET was stimulatory (*A* and *B*), inhibitory (*D*), or without effect (*C*) in different mutants.

Results

Effects of Charged MTS Reagents on Macroscopic Currents—Previously, we used internal application of charged MTS reagents to identify cytoplasmically accessible cysteine side chains introduced into different TMs (25, 26, 28, 38) as well as ICL3 (11). Here we used a similar approach to identify accessible side chains close to the putative cytoplasmic portals that were proposed by Mornon *et al.* (7), the approximate locations of which are illustrated in Fig. 1. Fig. 2 shows the effect of internal MTSES and MTSET on currents carried by several mutant channels in inside-out membrane patches during voltage ramps as well as the time course of current change monitored at −50

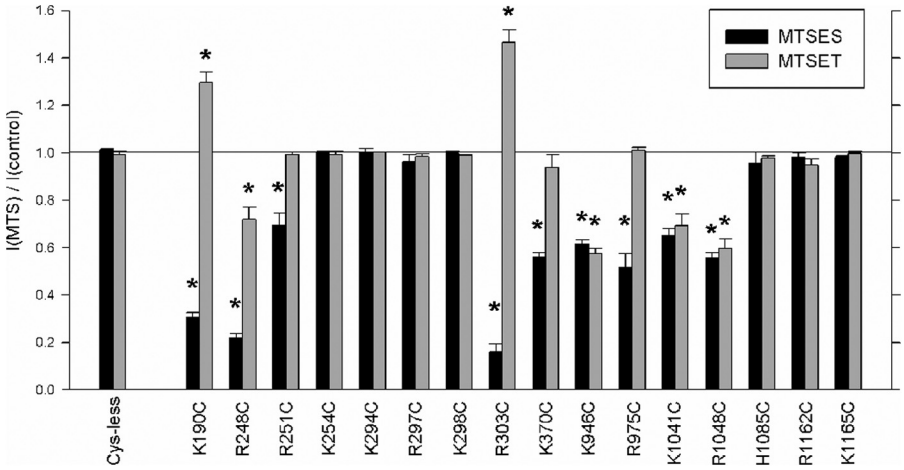

FIGURE 3. **Mean effect of MTS reagents on macroscopic current amplitude in different cysteine mutants.** For each channel variant studied, *black bars* represent the mean effect of MTSES, and *gray bars* represent the effect of MTSET (200 μM in each case) on macroscopic current amplitude at −50 mV. *Asterisks* indicate a significant difference from Cys-less ($p < 0.01$). *Error bars* represent the means ± S.E. from three to five patches.

mV in these same membrane patches. Application of MTSES (200 μM) following channel activation with PKA and ATP never caused an increase in macroscopic current amplitude but decreased current amplitude in K190C, R248C, R251C, R303C, K370C, K946C, R975C, K1041C, and R1048C (Figs. 2 and 3). The effect of MTSET on these MTSES-sensitive mutants was to increase (K190C and R303C), decrease (R248C, K946C, K1041C, and R1048C), or have no effect (R251C, K370C, and R975C) on macroscopic current amplitude (Figs. 2 and 3). Other mutants studied (K254C, K294C, R297C, K298C, H1085C, R1162C, and K1165C) were not significantly affected by either MTSES or MTSET (Fig. 3), suggesting that cysteine side chains at these positions were not modified by cytoplasmic MTS reagents. We did not observe any ATP- and PKA-dependent, $CFTR_{inh}$-172-sensitive macroscopic currents in inside-out patches associated with R153C, H949C, or K978C (Fig. 3), most likely due to lack of channel expression in the membrane (11). These experiments therefore support the hypothesis that many positively charged amino acid side chains from different ICLs are exposed to the cytoplasm around the level of the putative cytoplasmic portals to the pore.

The effects of MTS modification of side chains within the ICLs could reflect changes in Cl^- conductance (as suggested previously for R303C (19)) or in open probability (as shown previously for K946C and R975C (11)) or a combination of the two. In an attempt to isolate effects on Cl^- conductance at the macroscopic current level, we compared the effects of MTSES and MTSET on PKA- and ATP-activated currents from channels that are presumably gating normally (Fig. 2) with those on channels that had been activated with PKA and ATP and subsequently treated with 2 mM PP_i to promote channel "locking" in the open state (see "Experimental Procedures") (Fig. 4). Results with R303C, K946C, and R975C, which as described above are expected to affect predominantly Cl^- conductance (R303C) or gating (K946C and R975C), suggest that use of PP_i in this way can effectively separate effects on Cl^- conductance from those on gating. Thus, the effects of MTSES and MTSET on R303C were preserved following PP_i treatment, consistent with a gating-independent effect on Cl^- conductance (Figs. 4 and 5). In contrast, the effects of MTS reagents on both K946C and R975C were lost following PP_i treatment (Fig. 5), consistent with these reagents modifying the normal gating process (reducing channel open probability) without affecting Cl^- conductance (11). The effects of MTS reagents on R251C were similarly lost following PP_i treatment, suggesting that this mutant also had little or no effect on Cl^- conductance (Fig. 5). Inhibitory effects of MTS reagents on K1041C were diminished but not completely abolished following PP_i treatment (Fig. 5). In contrast, the inhibitory effects of MTSES on K190C, R248C, K370C, and R1048C were preserved following PP_i treatment (Figs. 4 and 5), suggesting that modification with this negatively charged reagent caused a major inhibition of Cl^- conductance in open channels in each of these mutants. Interestingly, in each of these four mutants, MTSET caused a significant increase in macroscopic current amplitude when applied after PP_i treatment (Figs. 4 and 5) even though MTSET applied in the absence of PP_i treatment decreased macroscopic current amplitude in R248C, K370C, and R1048C (Figs. 4 and 5). This implies that modification with positively charged MTSET caused an increase in Cl^- conductance in each of K190C, R248C, R303C, K370C, and R1048C, an effect that may potentially be masked by inhibitory effects on channel open probability in normally gating channels.

Effects of Mutations and Modifications on Single Channel Current Amplitude—To investigate more directly the involvement of positively charged amino acid side chains in the ICLs in contributing to the Cl^- permeation pathway, all MTS-sensitive cysteine mutants identified in Fig. 2 were also investigated using single channel recording. Unitary current amplitude was monitored at −50 mV both under control conditions and following exposure to MTSES or MTSET (Fig. 6). As described previously (11) and consistent with results from macroscopic current recording following channel treatment with PP_i (Fig. 5), application of MTSES or MTSET had no effect on current amplitude in K946C or R975C (Figs. 6 and 7). Current amplitude in R251C was slightly increased by MTSET but not significantly altered by MTSES (Figs. 6 and 7). In contrast, exposure to MTS reagents had strongly charge-dependent effects on cur-

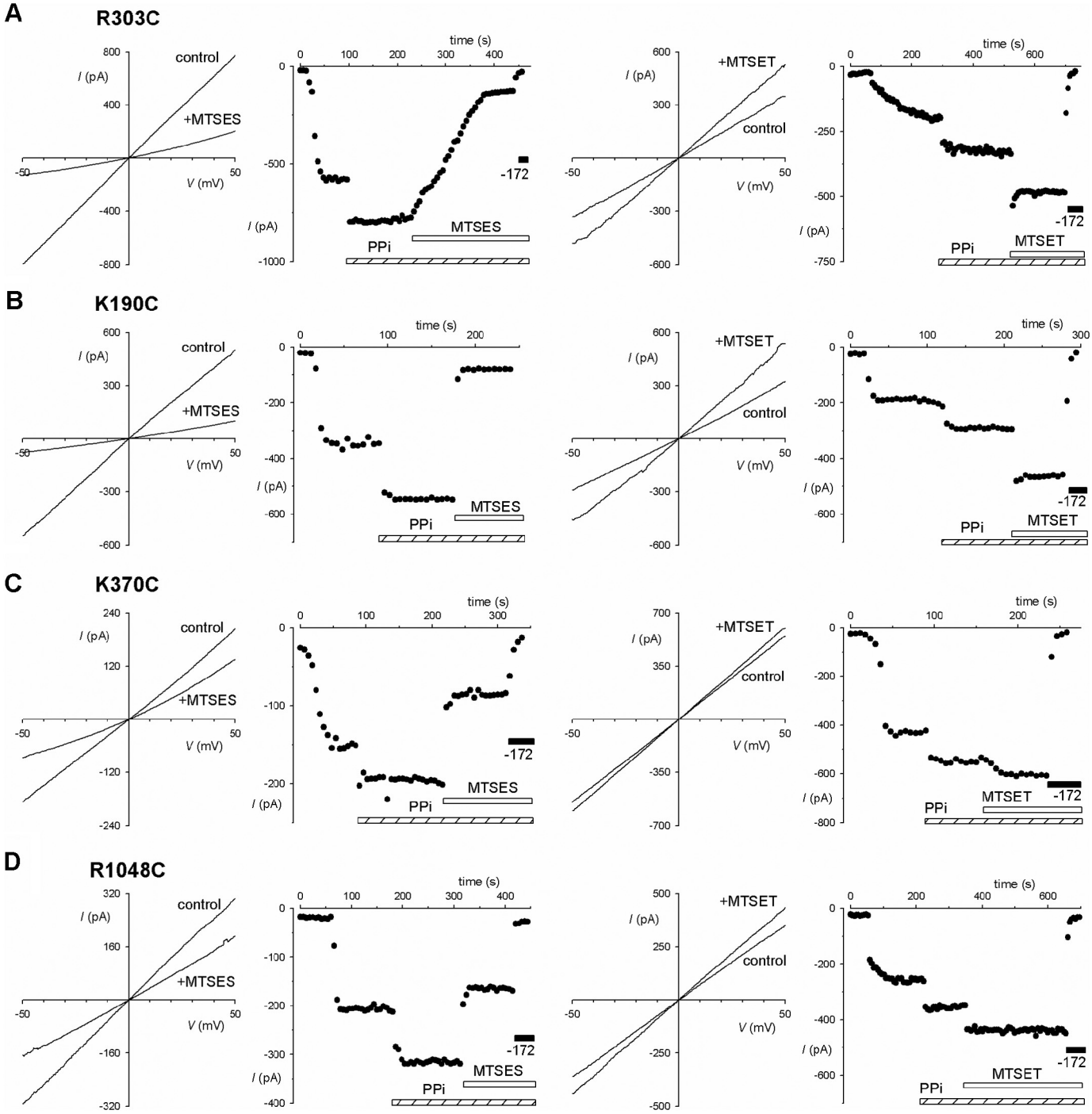

FIGURE 4. **Modification by cytoplasmically applied MTSES and MTSET following channel treatment with PP_i.** *A–D*, examples of modification of the same four mutants shown in Fig. 2 by MTSES (*left panels*) or MTSET (*right panels*). Following channel activation with PKA and ATP, channels were "locked" in the open state by application of PP_i (2 mM; as indicated by *hatched bars*) prior to addition of MTS reagent (200 μM; as indicated by *white bars*). The identity of CFTR currents was confirmed by sensitivity to $CFTR_{inh}$-172 (*-172*; 5 μM; indicated by *black bars*) at the end of the recording except for very small residual currents for K190C following MTSES modification. Note that for each of these mutants under these conditions the effect of MTSES was inhibitory, and that of MTSET was stimulatory.

rent amplitude in each of K190C, R248C, R303C, K370C, K1041C, and R1048C. In each of these six mutants, MTSES exposure significantly reduced current amplitude (Figs. 6 and 7*B*), and MTSET significantly increased current amplitude (Figs. 6 and 7*C*), leading to a clear dependence of current amplitude on side chain charge at each of these six positions (Fig. 6*C*). Interestingly, for each of these six mutants, unitary current amplitude in the absence of MTS reagents was significantly less than for Cys-less CFTR (Fig. 6 and 7*A*), suggesting that the removal of a positive charge associated with mutation to cysteine itself caused a reduction in Cl^- conductance. Consistent with this, restoration of the native positive charge following reaction with MTSET restored current amplitude to near Cys-less levels (Fig. 6). Overall the rank order of unitary current

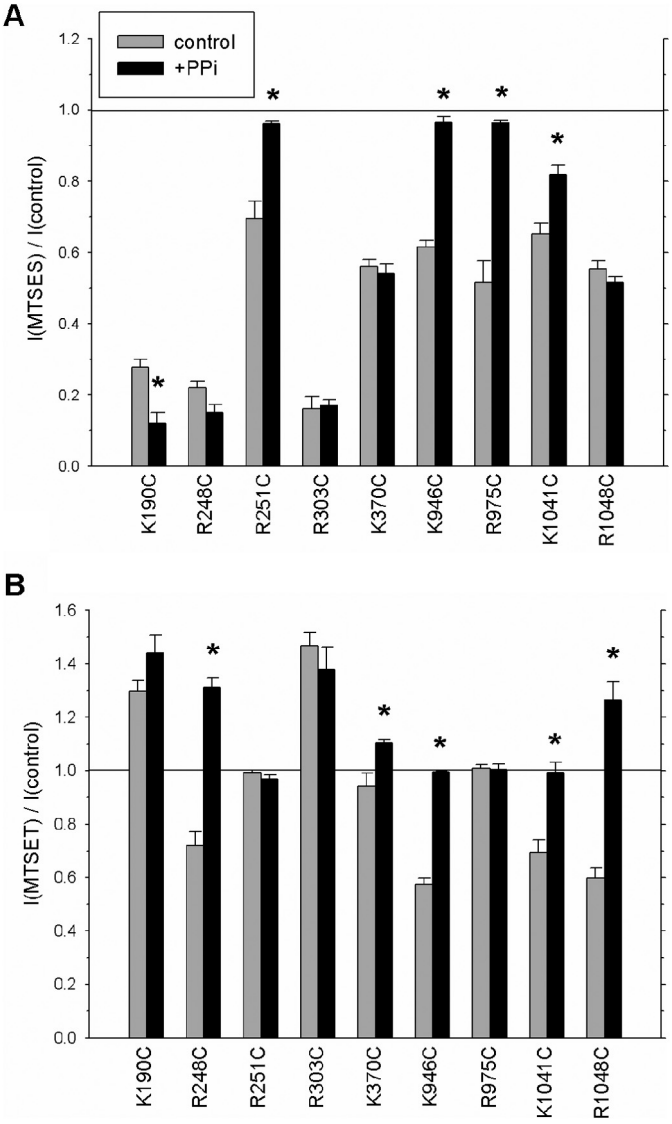

FIGURE 5. **Effect of treatment with PP_i on the effects of MTS reagents on macroscopic current amplitude in different cysteine mutants.** The mean effect of MTSES (*A*) and MTSET (*B*) (200 μM in each case) on macroscopic current amplitude at −50 mV is shown. In each case, *gray bars* represent currents recorded in the present of ATP and PKA alone, and *black bars* represent currents recorded following treatment with PP_i (2 mM) in the presence of ATP and PKA. *Asterisks* indicate a significant difference between control and PP_i-treated conditions ($p < 0.05$). *Error bars* represent the means ± S.E. from three to five patches.

amplitudes in unmodified channels was Cys-less ~ K946C ~ R975C > K370C > R251C > K1041C ~ R248C > R1048C > R303C > K190C (Fig. 7*A*). Among channels showing MTSES-sensitive current amplitudes, the order following modification was K1041C > R1048C > K370C > R248C > R303C > K190C (Fig. 6, *B* and *C*, and 7*B*).

Discussion

In contrast to all its ABC protein relatives, CFTR is an ion channel that allows electrodiffusional transmembrane movement of Cl^- and other small anions. This means that the CFTR protein has an open state in which a continuous pathway allows the movement of Cl^- between intracellular and extracellular solutions. Substituted cysteine accessibility mutagenesis studies (8) have identified amino acid residues in several TM and extracellular loop regions that appear to have side chains that line a continuous pathway from the extracellular solution to the inner ends of the TMs (Fig. 1*C*). Structure-function studies further support important functional roles for residues in the TMs and extracellular loops in contributing to the function of different parts of the CFTR Cl^- channel pore such as the outer vestibule, narrow region, and inner vestibule (4). Thus, the last remaining "gray area" of the anion permeation pathway is therefore the region between the intracellular ends of the TMs and the cytoplasm. Our present work identified a number of amino acid side chains in the ICLs that may play important roles in the electrostatic attraction of intracellular anions to the pore during epithelial cell anion secretion and thereby suggests a likely location of the cytoplasmic entrance to the pore.

Using substituted cysteine accessibility mutagenesis, we identified several amino acid side chains in the ICLs that are accessible to the intracellular solution (Fig. 3): Lys-190 (cytoplasmic extension to TM3), Arg-248 (TM4), Arg-251 (TM4), Arg-303 (TM5), Lys-370 (TM6), Lys-946 (TM8), Arg-975 (TM9), Lys-1041 (TM10), and Arg-1048 (TM10) (Table 1). This supports the idea that these extensions of the TM α-helices into the ICLs, which are located on the cytoplasmic side of the membrane, are relatively widely accessible to the intracellular solution. In contrast, other nearby residues were not modified by cytoplasmic MTS reagents following cysteine mutagenesis, namely Lys-254 (TM4), Lys-294 (TM5), Arg-297 (TM5), Lys-298 (TM5), His-1085 (TM11), Arg-1162 (TM12), and Lys-1165 (TM12) (Table 1). Although it is possible that these side chains could be accessible to the intracellular solution but that MTS modification was without functional effect, it is more likely that these side chains are simply inaccessible to MTS reagents especially because they were not functionally modified by either MTSES or MTSET.

Modification of exposed cysteine side chains by MTS reagents could result in a change in the rate of Cl^- movement and/or a change in channel open probability. To identify those residues that contribute to the Cl^- permeation pathway, we wished to identify those mutants in which MTS modification caused a charge-dependent change in Cl^- conductance. Single channel recording indicated directly that for each of K190C, R248C, R303C, K370C, K1041C, and R1048C Cl^- conductance was reduced relative to Cys-less (Figs. 6 and 7*A*), Cl^- conductance was further reduced by modification by negatively charged MTSES (Figs. 6 and 7*B*), and Cl^- conductance was restored to near wild-type (Cys-less) values by modification by positively charged MTSET (Figs. 6 and 7*C*). Thus, at each of these six positions, Cl^- conductance is determined by side chain charge (Fig. 6*C*), being maximal when a positive charge is present (in Cys-less or following modification by MTSET), reduced when the positive charge is removed by mutagenesis to cysteine, and reduced further still when a negative charge is introduced by modification by MTSES. This supports the idea that each of these six positively charged amino acid side chains normally acts to attract cytoplasmic Cl^- ions to the intracellular entrance to the pore in an electrostatic fashion, thus enhancing the ability of the channel effectively to transport Cl^- ions across the membrane to the extracellular solution (Table 1).

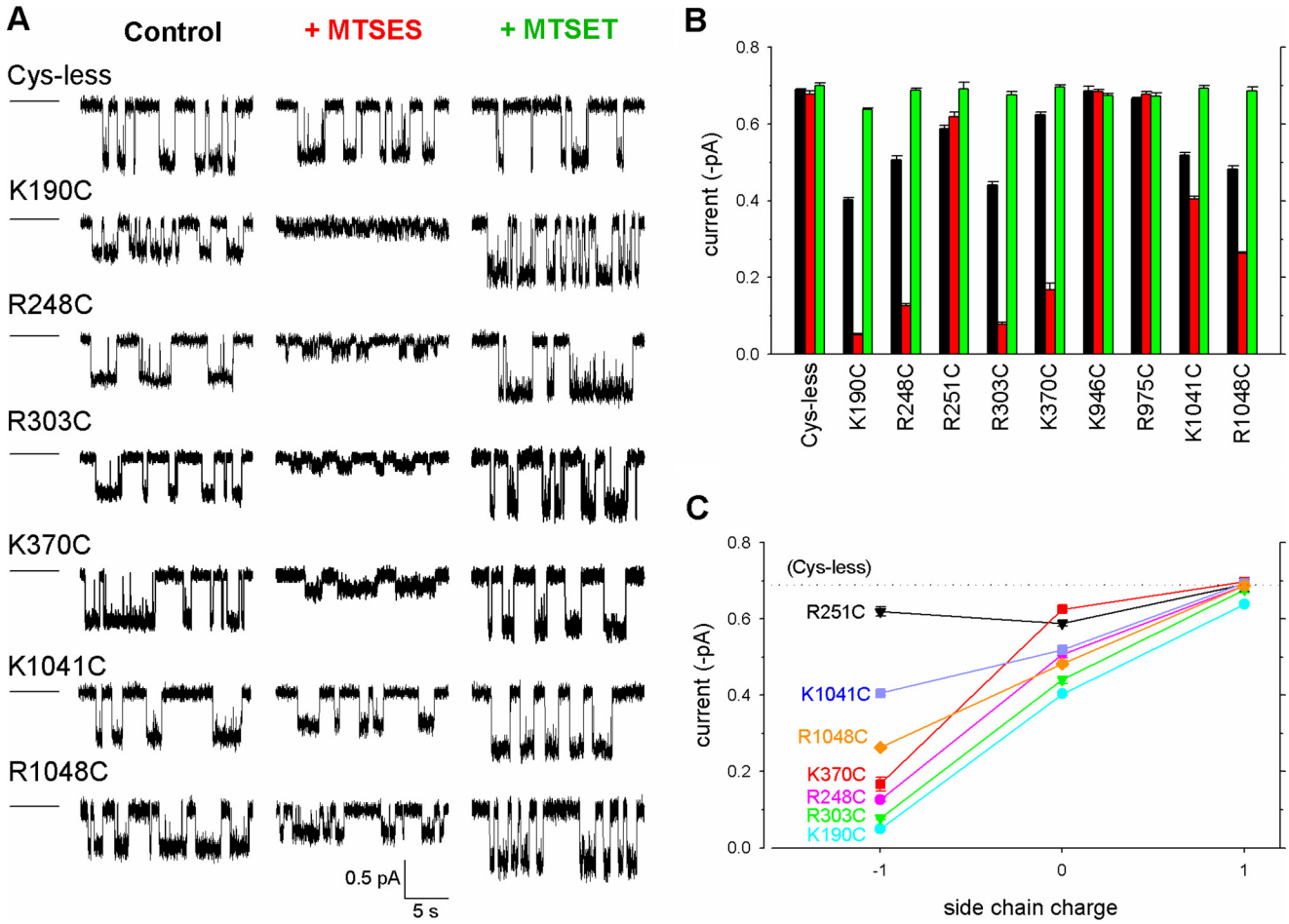

FIGURE 6. **Effects of MTS modification on single channel current amplitude.** *A*, example single channel currents recorded for the CFTR variants named at a membrane potential of −50 mV under control conditions (*black*; *left* traces) or following modification by MTSES (*red*; *center* traces) or MTSET (*green*; *right* traces). The closed state is indicated by the *line* to the *left* in each case. *B*, mean unitary current amplitude measured in each of these conditions for different channel variants. As in *A*, *black* represents control conditions, *red* represents following modification by MTSES, and *green* represents following modification by MTSET. *C*, mean unitary current amplitude in MTS-sensitive mutant channels as a function of presumed side chain charge (−1 following MTSES modification; 0 in unmodified channels, ignoring the potential partial negative charge of the cysteine side chain; and +1 following MTSET modification). *Error bars* represent the means ± S.E. from 3–10 patches.

Single channel recording evidence did not support a strong role for other cytoplasmically accessible positively charged side chains (Arg-251, Lys-946, and Arg-975) in electrostatic attraction of intracellular Cl^- ions to the pore (Figs. 6 and 7). Consistent with this, the functional effect of MTS reagents on R251C, K946C, and R975C were abolished in channels that had been treated with PP_i to maintain the channels in the open state (Fig. 5). This suggests that MTS modification of these mutants may have affected channel gating, leading to a change in overall macroscopic current amplitude (Fig. 3), as previously demonstrated directly for K946C and R975C using single channel recording (11). In contrast, the effects of MTS modification of PP_i-treated channels in K190C, R248C, R303C, K370C, and R1048C (Fig. 5) closely mirrored the charge-dependent effects of MTS modification on single channel current amplitude (Figs. 6 and 7). Only in K1041C was there a discrepancy between MTS effects on single channel current amplitude and on macroscopic current amplitude following PP_i treatment. This suggests that in most cases PP_i treatment can be used effectively to separate effects on Cl^- permeation (isolated in PP_i-treated channels) from those on channel gating (lost following PP_i treatment). Effects of MTS modification on channel gating were not investigated in detail here because our focus was on identification of amino acids that contribute to the Cl^- permeation pathway. Effects of both mutagenesis (12, 29–32) and MTS modification (including of K946C and R975C) (11) within the ICLs on channel gating have been reported previously; however, the mechanism(s) by which these manipulations of ICL structure affect channel gating is not well understood.

Recently, Mornon *et al.* (7) suggested, based on homology modeling and molecular dynamics simulations, that up to four lateral portals may connect the CFTR Cl^- channel pore with the cytoplasm at the level of the α-helical TM extensions that make up the ICLs (as illustrated in Fig. 1). The current work suggests that Lys-190, Arg-248, Arg-303, Lys-370, Lys-1041, and Arg-1048 all contribute to the electrostatic attraction of cytoplasmic Cl^- ions to the pore (Table 1 and Fig. 8*A*). We believe that the functional importance of Lys-190, Arg-248, Arg-303, and Lys-370 is likely greater than that of Lys-1041 and Arg-1048 because of the greater reduction in single channel current amplitude following introduction of a negative charge by MTSES modification in K190C, R248C, R303C, and K370C

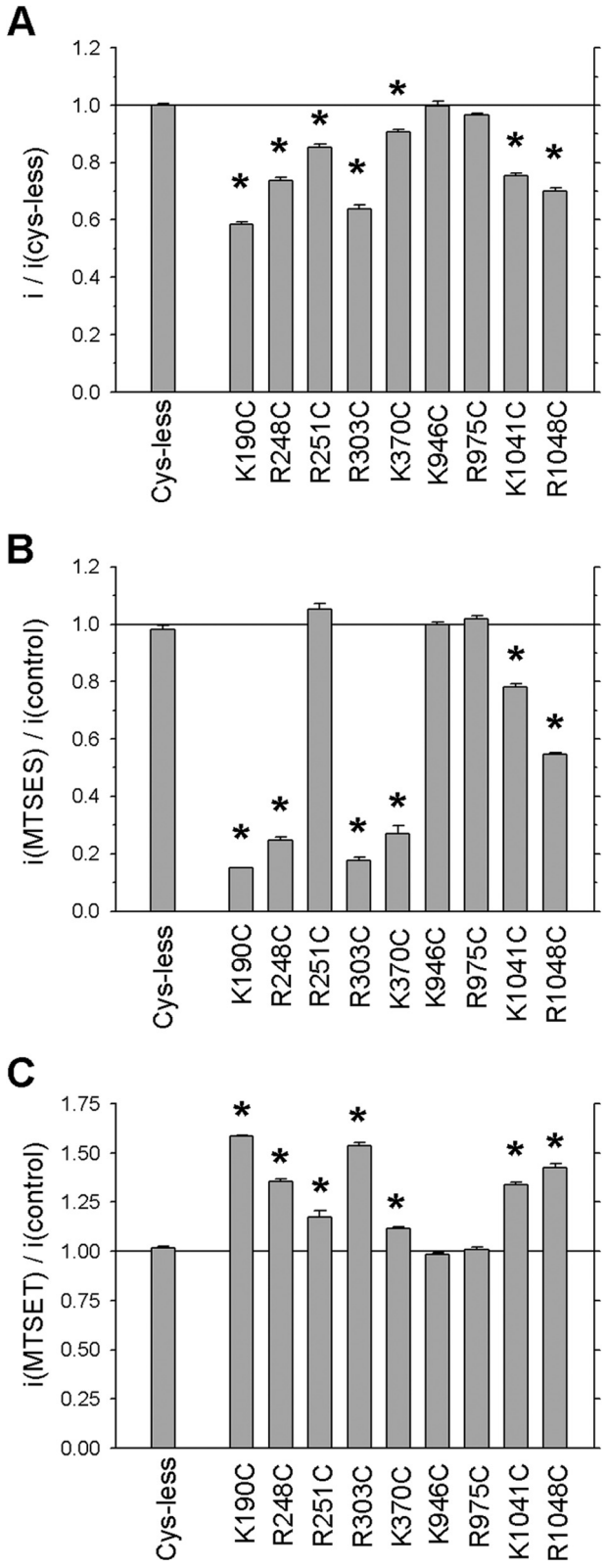

FIGURE 7. **Changes in single channel current amplitude in unmodified and modified channels.** *A*, mean unitary current amplitude at −50 mV as a fraction of that in Cys-less CFTR. *Asterisks* indicate a significant difference from Cys-less ($p < 0.00001$). *B*, mean effect of MTSES on unitary current amplitude at −50 mV. *C*, mean effect of MTSET on unitary current amplitude at −50 mV. In *B* and *C*, *asterisks* indicate a significant difference from current amplitude in the same channel variant in the absence of MTS reagent ($p < 0.0001$). In each panel, *error bars* represent the means ± S.E. from 3–10 patches.

TABLE 1

Exposure pattern of positively charged side chains based on modification of cysteine mutants by MTS reagents

As described in the text, sites at which cysteine modification altered Cl^- conduction are ascribed as pore-lining, those that were modified but for which no strong evidence for effects on Cl^- conduction was obtained are non-pore-lining, and those that were not modified are not exposed. The TM cytoplasmic extension for each residue is indicated.

Pore-lining		*Cytoplasmically-exposed but non-pore-lining*		*Not exposed*		*No functional expression*	
Lys-190	TM3	Arg-251	TM4	Lys-254	TM4	Arg-153	TM2
Arg-248	TM4	Lys-946	TM8	Lys-294	TM5	His-949	TM8
Arg-303	TM5	Arg-975	TM9	Arg-297	TM5	Lys-978†	TM9
Lys-370	TM6			Lys-298	TM5		
Lys-1041	TM10			His-1085	TM11		
Arg-1048	TM10			Arg-1162	TM12		
				Lys-1165	TM12		

† According to data presented in Wang *et al.* (32), Lys-978 should belong in the "cytoplasmically exposed but non-pore-lining" group. The failure of this mutant to express functional channels in our baby hamster kidney cell system, even though its functional properties had already been described by Wang *et al.* (32) using a different mammalian cell line expression system, has been discussed previously (11).

when compared with K1041C and R1048C (Figs. 6*C* and 7*B*). Single channel current amplitude was very low in MTSES-modified K190C, R248C, R303C, and K370C channels (<25% of Cys-less current amplitude; Figs. 6, *B* and *C*, and 7*B*), suggesting that most permeating Cl^- ions must pass close to these residues. Modification by MTSES had a lesser effect on unitary current amplitude in K1041C (~59% of Cys-less) and R1048C (~38% of Cys-less) (Fig. 6, *B* and *C*, and 7*B*) perhaps because these positive charges are located further from the major Cl^- permeation pathway. The four purportedly most functionally important pore-lining residues identified in the current work (Lys-190, Arg-248, Arg-303, and Lys-370) appear clustered around the TM4/TM6 entrance (Fig. 8), whereas Lys-1041 and Arg-1048 are expected to lie closer to the putative TM10/TM12 entrance (Fig. 8, *A* and *B*). The proposed locations of pore-forming positively charged side chains therefore suggests that a major entrance to the pore exists between TMs 4 and 6 with possibly a secondary entrance located between TMs 10 and 12 (Fig. 8*A*). Alternatively, it is possible that the relationship between charge at positions 1041 and 1048 and Cl^- conductance reflects the location of these side chains close to a central pore rather than close to any potential "secondary" portal because other positively charged residues close to the putative TM10/TM12 entrance (*i.e.* TM12 residues Arg-1162 and Lys-1165) do not appear to play important roles in electrostatic attraction of Cl^- ions (Fig. 8*A*). In contrast, our results do not provide evidence to support the idea that a functionally important "major lateral tunnel" (7) exists between TMs 2 and 11 and/or between TMs 5 and 8 (Figs. 1, *D* and *E*, and 8*A*).

When viewed from the side, these four functionally most important positively charged side chains can be seen to be located close to an apparent entrance to the central pore region between TMs 4 and 6 (Fig. 8*C*). We speculate that this apparent entrance may be the main lateral portal to the pore through which most if not all Cl^- ions enter the permeation pathway from the cytoplasm. Interestingly, positively charged residues located further toward the cytoplasmic ends of TM4 (Arg-251 and Arg-254) and TM5 (Lys-294, Arg-297, and Lys-298) were not found to be involved in Cl^- permeation, suggesting that the

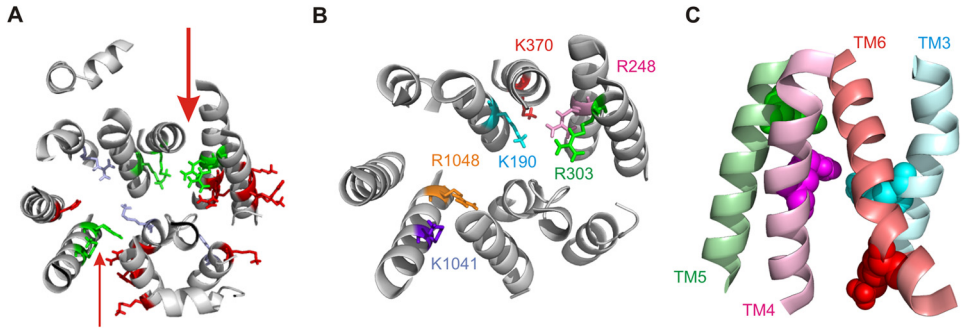

FIGURE 8. **Proposed location of pore-lining positively charged side chains.** *A*, homology structure of the ICLs viewed from the membrane side as in Fig. 1*D*. Positively charged side chains that are proposed to contribute to electrostatic attraction of Cl^- ions to the pore (Lys-190 in TM3, Arg-248 in TM4, Arg-303 in TM5, Lys-370 in TM6, and Lys-1041 and Arg-1048 in TM10) are shown in *green*. Other positively charged side chains for which we obtained no evidence for important interactions with Cl^- ions (Arg-251, Lys-254, Lys-294, Arg-297, Lys-298, Lys-946, Arg-975, His-1085, Arg-1162, and Lys-1165) are shown in *red*. Side chains for which we obtained no data due to lack of functional expression (Arg-153, His-949, and Lys-978) are shown in *blue*. Previously, it was suggested that Lys-978 did not interact strongly with Cl^- ions in the pore (32) (see also Table 1). The location of the proposed major portal between TM4 and TM6 is indicated by the *larger red arrow*. The location of a potential secondary portal between TM10 and TM12 is indicated by the *smaller red arrow*. *B* and *C*, more detailed view of proposed pore-forming side chains. *B*, same view as in *A*; peripheral cytoplasmic extensions to TMs 1 and 7 have been removed to allow a more detailed view. Coloring of different side chains is analogous to that used in Fig. 6*C*. *C*, view from the side (*i.e.* as if looking along the *larger red arrow* in *A*) of putative portal-lining cytoplasmic extensions to TMs 3, 4, 5, and 6. Side chains of Lys-190 (TM3), Arg-248 (TM4), Arg-303 (TM5), and Lys-370 (TM6) are shown as *space-filling* models using the same color scheme as the corresponding helical backbones to these TM extensions. As in Fig. 1, CFTR model structures were visualized with PyMOL (39) using coordinates provided by Mornon *et al.* (7).

lateral portal to the pore does not extend further into the cytoplasm.

In summary, our functional results support a role for fixed positive charges within the ICLs in electrostatic attraction of intracellular Cl^- ions to the cytoplasmic entrance to the pore to maximize the rate of Cl^- permeation. At the structural level, we suggest that Cl^- ions enter the pore via a lateral portal located between the cytoplasmic extensions of TM4 and TM6 and approximately at the level of TM6 residue Lys-370 (Fig. 8).

Acknowledgment—We thank Christina Irving for technical assistance.

References

1. Wang, Y., Wrennall, J. A., Cai, Z., Li, H., and Sheppard, D. N. (2014) Understanding how cystic fibrosis mutations disrupt CFTR function: from single molecules to animal models. *Int. J. Biochem. Cell Biol.* **52,** 47–57
2. Dean, M., Rzhetsky, A., and Allikmets, R. (2001) The human ATP-binding cassette (ABC) transporter superfamily. *Genome Res.* **11,** 1156–1166
3. Hwang, T.-C., and Kirk, K. L. (2013) The CFTR ion channel: gating, regulation, and anion permeation. *Cold Spring Harb. Perspect. Med.* **3,** a009498
4. Linsdell, P. (2014) Functional architecture of the CFTR chloride channel. *Mol. Membr. Biol.* **31,** 1–16
5. Cant, N., Pollock, N., and Ford, R. C. (2014) CFTR structure and cystic fibrosis. *Int. J. Biochem. Cell Biol.* **52,** 15–25
6. Odolczyk, N., and Zielenkiewicz, P. (2014) Molecular modeling approaches for cystic fibrosis transmembrane conductance regulator studies. *Int. J. Biochem. Cell Biol.* **52,** 39–46
7. Mornon, J.-P., Hoffmann, B., Jonic, S., Lehn, P., and Callebaut, I. (2015) Full-open and closed CFTR channels, with lateral tunnels from the cytoplasm and an alternative position of the F508 region, as revealed by molecular dynamics. *Cell. Mol. Life Sci.* **72,** 1377–1403
8. El Hiani, Y., and Linsdell, P. (2014) Conformational changes opening and closing the CFTR chloride channel: insights from cysteine scanning mutagenesis. *Biochem. Cell Biol.* **92,** 481–488
9. Mornon, J.-P., Lehn, P., and Callebaut, I. (2009) Molecular models of the open and closed states of the whole human CFTR protein. *Cell. Mol. Life Sci.* **66,** 3469–3486
10. Billet, A., Mornon, J.-P., Jollivet, M., Lehn, P., Callebaut, I., and Becq, F. (2013) CFTR: effect of ICL2 and ICL4 amino acids in close spatial proximity on the current properties of the channel. *J. Cyst. Fibros.* **12,** 737–745
11. El Hiani, Y., and Linsdell, P. (2012) Role of the juxtamembrane region of cytoplasmic loop 3 in the gating and conductance of the cystic fibrosis transmembrane conductance regulator chloride channel. *Biochemistry* **51,** 3971–3981
12. Wang, W., Roessler, B. C., and Kirk, K. L. (2014) An electrostatic interaction at the tetrahelix bundle promotes phosphorylation-dependent cystic fibrosis transmembrane conductance regulator (CFTR) channel opening. *J. Biol. Chem.* **289,** 30364–30378
13. Rosenberg, M. F., O'Ryan, L. P., Hughes, G., Zhao, Z., Aleksandrov, L. A., Riordan, J. R., and Ford, R. C. (2011) The cystic fibrosis transmembrane conductance regulator (CFTR). Three-dimensional structure and localization of a channel gate. *J. Biol. Chem.* **286,** 42647–42654
14. Miyazawa, A., Fujiyoshi, Y., Stowell, M., and Unwin, N. (1999) Nicotinic acetylcholine receptor at 4.6 Å resolution: transverse tunnels in the channel wall. *J. Mol. Biol.* **288,** 765–786
15. Gulbis, J. M., Zhou, M., Mann, S., and MacKinnon, R. (2000) Structure of the cytoplasmic β subunit-T1 assembly of voltage-dependent K^+ channels. *Science* **289,** 123–127
16. Payandeh, J., Scheuer, T., Zheng, N., and Catterall, W. A. (2011) The crystal structure of a voltage-gated sodium channel. *Nature* **475,** 353–358
17. Samways, D. S., Khakh, B. S., Dutertre, S., and Egan, T. M. (2011) Preferential use of unobstructed lateral portals as the access route to the pore of human ATP-gated ion channels (P2X receptors). *Proc. Natl. Acad. Sci. U.S.A.* **108,** 13800–13805
18. Carland, J. E., Cooper, M. A., Livesey, M. R., Hales, T. G., Peters, J. A., and Lambert, J. J. (2013) Mutagenic analysis of the intracellular portals of the human 5-HT_{3A} receptor. *J. Biol. Chem.* **288,** 31592–31601
19. St. Aubin, C. N., and Linsdell, P. (2006) Positive charges at the intracellular mouth of the pore regulate anion conduction in the CFTR chloride channel. *J. Gen. Physiol.* **128,** 535–545
20. St. Aubin, C. N., Zhou, J.-J., and Linsdell, P. (2007) Identification of a second blocker binding site at the cytoplasmic mouth of the cystic fibrosis transmembrane conductance regulator chloride channel pore. *Mol. Pharmacol.* **71,** 1360–1368
21. Mense, M., Vergani, P., White, D. M., Altberg, G., Nairn, A. C., and Gadsby, D. C. (2006) *In vivo* phosphorylation of CFTR promotes formation of a nucleotide-binding domain heterodimer. *EMBO J.* **25,** 4728–4739
22. Li, M.-S., Demsey, A.F., Qi, J., and Linsdell, P. (2009) Cysteine-independent inhibition of the CFTR chloride channel by the cysteine-reactive reagent sodium (2-sulphonatoethyl)methanethiosulphonate (MTSES).

Br. J. Pharmacol. **157,** 1065–1071
23. Holstead, R. G., Li, M.-S., and Linsdell, P. (2011) Functional differences in pore properties between wild-type and cysteine-less forms of the CFTR chloride channel. *J. Membr. Biol.* **243,** 15–23
24. Zhou, J.-J., Li, M.-S., Qi, J., and Linsdell, P. (2010) Regulation of conductance by the number of fixed positive charges in the intracellular vestibule of the CFTR chloride channel pore. *J. Gen. Physiol.* **135,** 229–245
25. El Hiani, Y., and Linsdell, P. (2010) Changes in accessibility of cytoplasmic substances to the pore associated with activation of the cystic fibrosis transmembrane conductance regulator chloride channel. *J. Biol. Chem.* **285,** 32126–32140
26. Wang, W., El Hiani, Y., and Linsdell, P. (2011) Alignment of transmembrane regions in the cystic fibrosis transmembrane conductance regulator chloride channel pore. *J. Gen. Physiol.* **138,** 165–178
27. El Hiani, Y., and Linsdell, P. (2014) Metal bridges illuminate transmembrane domain movements during gating of the cystic fibrosis transmembrane conductance regulator chloride channel. *J. Biol. Chem.* **289,** 28149–28159
28. Wang, W., El Hiani, Y., Rubaiy, H. N., and Linsdell, P. (2014) Relative contribution of different transmembrane segments to the CFTR chloride channel pore. *Pflügers Arch.* **466,** 477–490
29. Seibert, F. S., Linsdell, P., Loo, T. W., Hanrahan, J. W., Clarke, D. M., and Riordan, J. R. (1996) Disease-associated mutations in the fourth cytoplasmic loop of cystic fibrosis transmembrane conductance regulator compromise biosynthetic processing and chloride channel activity. *J. Biol. Chem.* **271,** 15139–15145
30. Cotten, J. F., Ostedgaard, L. S., Carson, M. R., and Welsh, M. J. (1996) Effect of cystic fibrosis-associated mutations in the fourth intracellular loop of cystic fibrosis transmembrane conductance regulator. *J. Biol. Chem.* **271,** 21279–21284
31. Seibert, F. S., Linsdell, P., Loo, T. W., Hanrahan, J. W., Riordan, J. R., and Clarke, D. M. (1996) Cytoplasmic loop three of cystic fibrosis transmembrane conductance regulator contributes to regulation of chloride channel activity. *J. Biol. Chem.* **271,** 27493–27499
32. Wang, W., Wu, J., Bernard, K., Li, G., Wang, G., Bevensee, M. O., and Kirk, K. L. (2010) ATP-independent CFTR channel gating and allosteric modulation by phosphorylation. *Proc. Natl. Acad. Sci. U.S.A.* **107,** 3888–3893
33. Serohijos, A. W., Hegedus, T., Aleksandrov, A. A., He, L., Cui, L., Dokholyan, N. V., and Riordan, J. R. (2008) Phenylalanine-508 mediates a cytoplasmic-membrane domain contact in the CFTR 3D crystal structure crucial to assembly and channel function. *Proc. Natl. Acad. Sci. U.S.A.* **105,** 3256–3261
34. Gunderson, K. L., and Kopito, R. R. (1994) Effects of pyrophosphate and nucleotide analogs suggest a role for ATP hydrolysis in cystic fibrosis transmembrane conductance regulator channel gating. *J. Biol. Chem.* **269,** 19349–19353
35. Carson, M. R., Winter, M. C., Travis, S. M., and Welsh, M. J. (1995) Pyrophosphate stimulates wild-type and mutant cystic fibrosis transmembrane conductance regulator Cl^- channels. *J. Biol. Chem.* **270,** 20466–20472
36. Wang, W., and Linsdell, P. (2012) Conformational change opening the CFTR chloride channel pore coupled to ATP-dependent channel gating. *Biochim. Biophys. Acta* **1818,** 851–860
37. Wang, W., and Linsdell, P. (2012) Alternating access to the transmembrane domain of the ATP-binding cassette protein cystic fibrosis transmembrane conductance regulator (ABCC7). *J. Biol. Chem.* **287,** 10156–10165
38. Qian, F., El Hiani, Y., and Linsdell, P. (2011) Functional arrangement of the 12th transmembrane region in the CFTR chloride channel pore based on functional investigation of a cysteine-less CFTR variant. *Pflügers Arch.* **462,** 559–571
39. DeLano, W. L. (2010) *The PyMOL Molecular Graphics System*, version 1.3r1, Schrödinger, LLC, New York